A dynamic airspace grid map based on 3D subdivision framework

Bing Han [1], Tengteng Qu [2]

[1] Academy for Advanced Interdisciplinary Studies, Peking University, Beijing 100871, China - hanbing@stu.pku.edu.cn
[2] College of Engineering, Peking University, Beijing 100871, China - tengteng.qu@pku.edu.cn

Keywords: Airspace map, GeoSOT-3D, Discrete grid, Time-variance, 3D subdivision.

Abstract

This paper proposes a dynamic airspace grid map based on a 3D subdivision framework to address the lack of standardized modeling framework in current spatial management, difficulties in finely managing small scale areas, and low efficiency issues. The dynamic airspace grid map adopts the GeoSOT-3D subdivision framework, which can seamlessly encode and manage the three-dimensional spatial domain at multiple levels without stacking. Grid map also models static and dynamic airspace, including obstacles, dynamic airspace attributes, aircraft, and can achieve intelligent visualization of time- variance airspace. Finally, the dynamic airspace grid map can organize and store static and dynamic spatial data based on a 3D subdivision framework to ensure the orderliness and security of the airspace domain.

1. Introduction

Airspace refers to any area and space on the Earth's surface that can provide for civil aircraft to fly (Kwon, Kim, and Choi 2018). With the increasing airspace traffic flow and number of unmanned aerial vehicles (UAVs) in recent years, it is particularly important to allocate and utilize airspace resources more reasonably and effectively. Among them, the construction of airspace maps is the foundation of practical applications such as airspace digital twin, intelligent mobility, autonomous flight, and traffic control (Bauranov, and Rakas 2021; Pang et al., 2020). However, the current airspace map mainly has some problems need to be addressed, such as lack of standardized modeling framework, difficulties in finely managing small-scale areas, and low efficiency in manual airspace delineation (Hearn, Kotwicz Herniczek, and German 2023).

The dynamic airspace division lacks uniformity and completeness (LIAO, XU, and YE 2024). There is a huge demand for the development of general aviation and unmanned aerial vehicles in the airspace. How to establish an airspace planning model that includes airspace information is a fundamental issue in current research. Consistency is reflected in the model's applicability to dynamic low altitude airspace worldwide, while integrity is reflected in the comprehensive data information of dynamic low altitude ground and airspace. Meanwhile, the current airspace partitioning methods are unable to finely model small-scale regions (Huang, Su, and Wang 2024). For a long time, due to the lack of structural description, airspace delineation has been unable to organize three-dimensional geographic location identification, spatial environment data, and dynamic flight information in a spatial manner (Guan et al., 2024). The current modeling method for boundaries cannot meet the high dynamic changes in future airspace, and there is an urgent need to solve the problem of unified modeling and expression of airspace boundaries and interiors (Li et al., 2010).

In addition, it is difficult to achieve real-time planning in the airspace, and there is a large amount of manual work involved (Xie et al., 2024). In the existing airspace management system, manual control plays an extremely important role. In the context of the development of open low altitude airspace, low altitude airspace will face a large influx of aircraft and an increasing demand for flight tasks (Davies et al., 2021). Through manual control and coordination, the workload of control personnel will rapidly increase and the safety of low altitude airspace will be reduced. It is urgent to introduce an automated dynamic airspace situation map to assist controllers in management and decision-making (Sainz Carreño et al., 2023).

Therefore, this paper provides a method for constructing a dynamic airspace situation map based on a three-dimensional grid. In response to the existing needs of unified and integrated management, the vigorous development of general aviation and unmanned aerial vehicle industries, and safe flight in dynamic airspace, the airspace is uniformly divided into multi-scale three-dimensional grid grids to achieve effective integration of grids and entities, which provides technical support for the dynamic and intelligent modeling of airspace situation maps through grid (Zhao et al., 2024).

2. 3D subdivision framework

In this paper, GeoSOT-3D (Geographic Coordinate Subdividing Grid with One Dimension Integrated Coding on 2^n Tree-3D) is selected as the coding scheme for 3D subdivision framework to establish an abstract environment (Zhai et al., 2021), as shown in Figure 1. The subdivision of GeoSOT-3D is to expand the latitude and longitude to a space of 512 °× 512 °, and use the equal latitude and longitude recursive quadtree partitioning method to perform multi-scale subdivision on the expanded space. The altitude is mapped to 512 degrees, corresponding to the airspace range from an altitude of 50000 kilometers to the center of the earth (Han et al., 2023; Han, Qu, and Jiang 2025). The GeoSOT-3D is a 32 level multi-scale octree solid grid that uniquely identifies and stores internal information for each discrete element in the spatial domain through grid encoding (Liu et al., 2022).

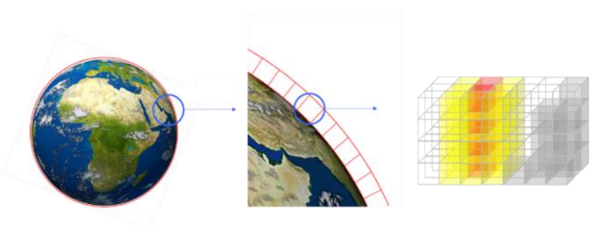

Figure 1. GeoSOT-3D earth subdivision grid for airspace map.

3. Dynamic airspace grid map modeling

Airspace can be divided into static airspace areas and dynamic airspace areas, such as flight information zones, control zones, danger zones, permanent restricted zones, etc., which are established for a long time and do not have a termination time without prior notice (Han et al., 2022). This type of airspace is called static airspace area; And most restricted areas, temporary restricted areas, etc. have termination times or duration periods, which are dynamic airspace areas. The Dynamic airspace grid map will discretize and model both types of airspace.

3.1 Static airspace

3.1.1 Static obstacles

Static obstacles refer to a large number of impassable obstacles, divided into natural obstacles and man-made obstacles. Natural obstacles include mountains, hills, trees, etc., while man-made obstacles include buildings, bridges, elevated roads, etc. Both have the characteristics of occupying a certain geographic 3D space and not undergoing displacement changes in a short period of time, so they are called static obstacles. The expression of static obstacles is divided into the following steps:
Step 1: Grid the obstacle object according to its geometric shape, with a mesh scale of the minimum level $L_{now}=L_{lowest}$;
Step 2: If the current level L_{now} is not the $L_{highest}$, then set the current higher level as the level to be aggregated. Based on the encoding structure of all the grids in the previous step, take the grid code of each grid's parent level and store it in the database;
Step 3: Repeat Step 2 until$L_{now}=L_{highest}$, indicating that the obstacle segmentation results have been aggregated into the highest-level grid. The expression process of static obstacles can be represented as Figure 2.

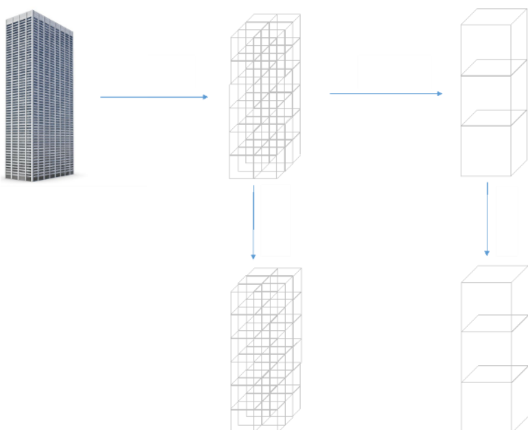

Figure 2. Schematic diagram of static obstacle grid representation.

3.1.2 Static airspace area

Static airspace areas mainly include flight information zones, control zones, etc., whose shapes coincide or are similar to the boundaries of provinces and cities, and are difficult to express through simple geometric functions. The grid representation of static airspace is divided into the following steps:
Step 1: Take a specific grid level and use grids at the same level to divide the spatial domain, including irregular static areas, to obtain a series of grids;
Step 2: Convert the latitude and longitude coordinates of the westernmost point P_W, northernmost point P_N, easternmost point PE, and southernmost point PS in the static area into grid codes to obtain the corresponding G_W, G_N, G_E, and G_S grids;
Step 3: Add the grid G_W to the boundary grid sequence $LIST_{border}$.
Step 4: Starting from the latest added grid G_{new} in the $LIST_{border}$, in the order of the eight neighborhood grids a to h, examine whether the coordinates of one or two boundary angles closest to G_{new} with a distance of ε are in the static area to be examined. If they exist, set the grid as G_{wait} and add the point to the $LIST_{border}$; If it does not exist, then investigate the next grid point in order until a point is found to exist and set as G_{wait}. If the first grid of the $LIST_{border}$ is not G_{wait}, add that point to the $LIST_{border}$ and repeat Step 3; Otherwise, the loop ends. The schematic diagram of the marginal grid expression in the static airspace area is shown in Figure 3.

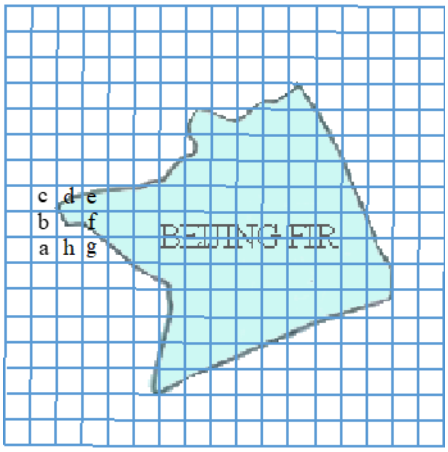

Figure 3. Schematic diagram of grid representation of static airspace area edges.

3.2 Dynamic airspace

The airspace map also needs to manage areas with specified durations and dynamically moving areas, which are called time-variance airspace areas (Du, Lu, and Wu 2020). The spatial location range of time-variance airspace remains unchanged, but it has duration regulations, such as most restricted areas, temporary restricted areas, etc. When organizing grid data for time-variance airspace, the duration needs to be identified. The dynamic airspace area includes a restricted area for drone flight, and its shape rules can be expressed through geometric functions. The grid representation of time-variance airspace first requires determining the shape of the time-variance airspace, and then determining the required information based on the shape characteristics.
The dynamic airspace grid map is mainly used to manage the airspace can fly in, abbreviated as flight airspace A_F. After grid subdivision, the flight airspace A_F assigns grid codes, with each grid g_d representing a specific airspace, to show the status and attributes of aircraft U_0, U_1, …, U_n. In the airspace map, the dynamic attributes of the airspace grid include grid occupancy, current grid capacity, and grid occupancy uniformity.

3.2.1 Grid occupancy

Whether the grid is occupied or not is one of the most important judgments in dynamic airspace maps. If there is an aircraft in the grid at a certain moment, the current grid is occupied. When expressing the dynamic grid map, the grid is filled with a warning color (red); If there is no aircraft in Ti at a certain moment in the grid, then the current grid is not occupied and is filled with a background color (white) in the dynamic situation map, that is:

$$occupation\_\, g_d = \begin{cases} 1 & U_i \ in \ g_d, \ \ t = T_i \\ 0 & g_d \ = \ \phi, \ \ t = T_i \end{cases}, \tag{1}$$

Where, all $occupation\_g_d$ values in the initial flight airspace are 0, indicating that the entire flight airspace is in an idle state. When the aircraft enters the airspace, real-time updates of the flight airspace begin. When the aircraft enters a certain grid, the $occupation\_g_d$ value of that grid is set to 1. When the aircraft leaves the grid, $occupation\_g_d$ returns to 0. Real time update calculation of grid occupancy for the entire flight airspace, that is, for the smallest scale flight airspace grid, calculate the current $occupation\_g_d$ of each grid and update it in real-time to the database, as shown in Figure 4.

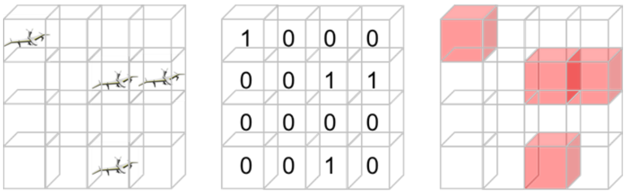

Figure 4. Schematic diagram of grid occupancy.

3.2.2 Current grid capacity

The current grid capacity represents the total number of aircraft Ti exists in the grid at a certain moment, which is of great significance in airspace flow management and flight mission planning, that is:

$$capacity\_g_d = \Sigma\, U_i \qquad U_i \ in \ g_d, \ \ t = T_i, \tag{2}$$

Where, the initial flight airspace's $capacity\_g_d$ is all 0, indicating that there are no aircraft in the entire flight airspace. When an aircraft enters the airspace, the number of aircraft in each flight airspace grid at a certain moment is added and the $capacity\_g_d$ is updated. When considering the expression of multi-scale flight airspace, the current capacity of large-scale grids can be obtained by adding up the current capacity of small-scale grids, that is:

$$capacity\_G_d = \Sigma\, capacity\_g_d \qquad g_d \ in \ G_d, \ \ t = T_i, \tag{3}$$

The current capacity of the large-scale grid $capacity\_G_d$ is the total number of aircraft obtained by accumulating the current capacity of all small-scale grids contained in the large-scale grid, and a threshold value I_{th} can be set as needed. When the current capacity of the grid $capacity\_G_d$ does not exceed the threshold value I_{th}, it is a low-capacity grid, and the grid is the background color when visualized; When the threshold I_{th} is exceeded, it is a high-capacity grid, and the grid appears as a warning color during visualization, as shown in Figure 5.

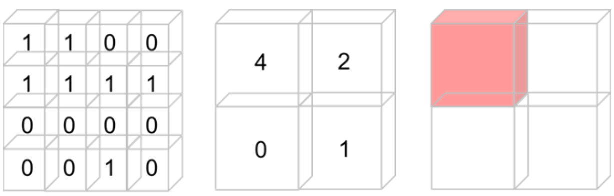

Figure 5. Schematic diagram of current grid capacity.

3.2.3 Grid occupancy uniformity

In large-scale grids, in addition to considering the current grid capacity, it is also necessary to consider the distribution of aircraft in the grid. As shown in Figure 6, the total number of aircraft in the four small grids on the left and the adjacent four small grids are the same, both at 40. This means that the current capacity of the large-scale grid is the same. However, the number of aircraft in the four small grids on the left is relatively average, while the adjacent four differ greatly. When planning paths or tasks, grids with zero or very few aircraft in the grid can be considered, but they are difficult to reflect at a large scale. The time consumption caused by splitting and refining all large-scale grids during planning is large, which does not meet the actual needs of dynamic real-time computing. Therefore, the concept of grid occupancy uniformity is introduced.

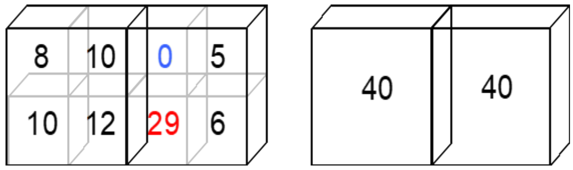

Figure 6. Comparison diagram of uniformly and unevenly distributed grids.

Grid occupancy uniformity refers to the distribution of aircraft in small-scale grids within a large-scale grid. When the distribution is relatively even, it can be understood that small-scale grids have equivalence. When the distribution is uneven, information such as the current capacity of small-scale grids can be extracted, and grids that meet the requirements can be further calculated. Grids with lower grid occupancy uniformity are often considered. The calculation method is as follows:

$$average\_G_d = \frac{\Sigma\, capacity\, g_d}{Ngd} \qquad g_d \ in \ G_d, \ \ t = T_i, \tag{4}$$

$$balance\_{G_d}^{\,2} = \frac{\Sigma\,(capacity\, g_d - average_{G_d})^2}{N_{g_d}} \qquad g_d \ in \ G_d, \ \ t = T_i, \tag{5}$$

When calculating the grid occupancy uniformity, first calculate the average value of the number of aircraft in the grid, which is called "$average\_G_d$". Then, calculate the difference between the current capacity of each small-scale grid $capacity\_G_d$, and the average value $average\_G_d$. Finally, the grid occupancy uniformity $balance\_G_d$ is obtained by adding and taking the square root, as shown in Figure 7.

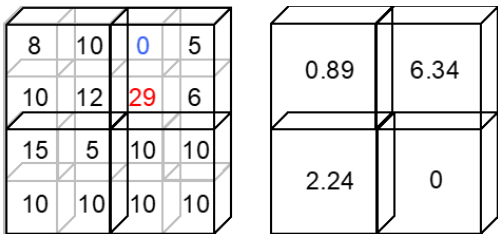

Figure 7. Schematic diagram of grid occupancy uniformity.

3.3 Aircraft

In dynamic airspace grid diagrams, aircraft are the most important component, which are represented as particles and buffer zones (Han et al., 2021).

3.3.1 Particles

The fuselage of an aircraft occupies multiple grids in the minimum scale grid situation map, especially in fixed wing aircraft and helicopter models. Recording the location of the aircraft is the most basic operation for route planning and information exchange. If a set of multiple grid codes is used to represent the location of a certain aircraft, it will cause complexity in data storage and information exchange. Therefore, this article abstracts the aircraft A_c as a particle Point_A_C, where the location of the particle is the physical center of gravity of the aircraft, and the location of the aircraft is the encoded Code_g_d of the grid where the particle is located, whose mathematical description is:

$$\begin{cases} Ac = \left(\cup_{i=1}^{n} Ac\_Code_{g_d}\right) \cup \left(\cup_{i=1}^{n} Ac\_Attr\right) \\ Point_{\_Ac} = Code_{g_d} \end{cases}, \tag{6}$$

Among them, $Ac\_Code_{g_d}$ represents the geometric occupancy grid of aircraft A_c, Ac_Attr represents the physical properties of aircraft A_c, A_c represents the set of geometric occupancy grids and the associated set of physical properties, and the position of the aircraft is the position of particle $Point_{\_Ac}$, represented as the Code_ g_d _d of the grid where the particle is located. The schematic diagram of the aircraft abstracted as a particle is shown in Figure 8.

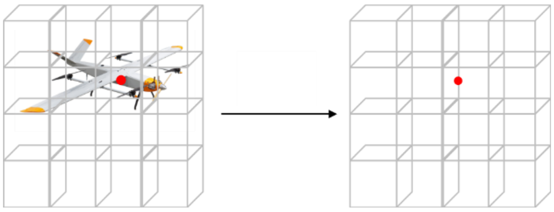

Figure 8. Schematic diagram of aircraft abstracted as particle.

3.3.2 Buffer zones

Describing aircraft as particles can facilitate position recording and data storage, but in some cases, ignoring the fuselage can pose safety hazards. For example, in the collision detection calculation process, two aircraft need to consider the values of fuselage length and height to avoid collision, and further minimum distance calculation needs to be carried out based on the speed of the two aircraft. Therefore, the concept of buffer zone is introduced. A buffer zone refers to the dynamic spatial range formed around an aircraft during its motion. Other aircraft cannot enter this area, otherwise it may pose a collision risk. The mathematical description of a buffer zone is:

$$\begin{cases} Buffer_x = LengthX_{Ac} + F(V\_Ac) \\ Buffer_y = LengthY_{Ac} + F(V\_Ac), \\ Buffer_z = LengthZ_{Ac} + F(V\_Ac) \end{cases} \tag{7}$$

Where $Buffer_x$, $Buffer_y$, and $Buffer_z$ are the component lengths of the buffer zone in three directions, $LengthX_{Ac}$ is the length of the aircraft body, $LengthY_{Ac}$ is the width of the aircraft body, $LengthZ_{Ac}$ is the height of the aircraft, and F(V_Ac) is a function of the aircraft speed V_Ac. The abstract expression diagram of the buffer zone is shown in Figure 9.

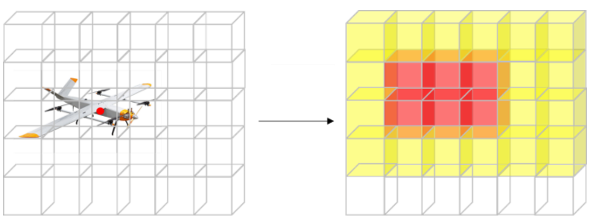

Figure 9. Schematic diagram of aircraft abstracted as buffer zone.

3.4 Time-variance airspace visualization

The dynamic airspace grid map also needs to specify rules for airspace updates. Each airspace update requires that the dynamic properties of all grids in the flight airspace be updated sequentially at each T_i moment, in the order of grid occupancy, current grid capacity, and grid occupancy uniformity. To meet the user's intuitive perception of the situation map while ensuring real-time computing efficiency and reducing rendering times, it is necessary to hide some detailed information at a large scale, such as the specific location and direction of movement of each aircraft, and represent the occupation and changes of airspace at a large scale through statistical information such as current grid capacity and grid occupancy uniformity. In extreme cases, it is necessary to update the dynamic properties of all grids in the flight airspace at each T_i moment. Therefore, dynamic airspace visualization is the presentation of the occupancy status of the flight airspace and the flight status of the aircraft in the form of a situational map to users. The visualization steps are as follows:

Step 1: Rendering all levels of grids in the flight airspace from the smallest scale to the largest scale, filling them with background colors, and initializing each grid's $occupation_{g_d}$, $capacity\_\,g_d$, and $balance\_\,G_d$ to 0;

Step 2: Extract the three-dimensional grid position codes of all aircraft in the flight airspace at time point Ti, fill the grid with a warning color (red), and add 1 to the $occupation\_\,g_d$ of the grid;

Step 3: For each grid with a change in $occupation\_\,g_d$, based on the scale correlation of the grid codes, the parent grid code is found layer by layer, and the $capacity\_\,g_d$ and $balance\_\,G_d$ of the parent grid are recalculated layer by layer. For parent grids with $capacity\_\,g_d$ below the set threshold I_{th}, the fill color becomes the background color, and for parent grids with $capacity\_\,g_d$ exceeding the set threshold I_{th}, the fill color becomes the warning color (red);

Step 4: When the occupancy $occupation_{g_d}$ of a certain grid in the flight airspace changes, the aircraft is triggered to recalculate the occupancy occupancy $occupation_{g_d}$ of the grid entering and leaving the grid, and update the $capacity\_\,g_d$ and $balance\_\,G_d$ of the parent grid layer by layer, repeating step 3.

4. Airspace data grid organization

4.1 Static data grid organization

The static airspace areas mainly include flight information zones, control zones, etc., whose forms coincide or are similar to the boundaries of provinces and cities. The data structure of its subdivision expression is shown in Table 1.

Region ID	Region type	Grid code west boundary	Grid code north boundary	Grid code east boundary	Grid code south boundary	Grid boundary sequence
Reg_ID1	TYPE1	LSGW_CODE1	LSGN_CODE1	LSGE_CODE1	LSGS_CODE1	LSG_CODE_List1
Reg_ID2	TYPE2	LSGW_CODE2	LSGN_CODE2	LSGE_CODE2	LSGS_CODE2	LSG_CODE_List2
Reg_ID3	TYPE3	LSGW_CODE3	LSGN_CODE3	LSGE_CODE3	LSGS_CODE3	LSG_CODE_List3
…	…	…	…	…	…	…
Reg_IDN	TYPE3	LSGW_CODEN	LSGN_CODEN	LSGE_CODEN	LSGW_CODEN	LSG_CODE_ListN
Reg_ID1	TYPE1	LSGW_CODE1	LSGN_CODE1	LSGE_CODE1	LSGS_CODE1	LSG_CODE_List1

Table 1. Static airspace grid representation data structure.

4.2 Dynamic data grid organization

Dynamic data organization is more complex than static data organization. Static data displays location and space, while dynamic data needs to display multiple information such as location, trajectory, and changes in airspace status, and the information is correlated. For example, trajectory data is obtained by accumulating location data and time points, and changes in airspace status are the overall manifestation of aircraft position changes.

Flight path refers to the flight route set for a certain aircraft based on starting, ending, and mission conditions. It is often necessary to plan and store it in a database before the aircraft takes off, and guide the aircraft to complete the mission during the flight process; The flight trajectory refers to the route that an aircraft continuously passes through during a certain period of time, and as a completed path, the trajectory also needs to be stored and analyzed Paths and trajectories have many similarities, so they can be expressed in a correlated manner when representing data structures. The path and trajectory are both grid sequences that record a series of grid codes for the aircraft entering and leaving during a certain period of time. The data structure for the grid representation of the path and trajectory is shown in Table 2.

Object ID	Starting time point	Current time point	Accumulated time	Start spatial grid code	Current spatial grid code	Path/trajectory	Task ID
Obj_ID 1	First_Time 1	Last_Time 1	Spend_Time 1	First_LSG_CODE 1	Last_LSG_CODE 1	LSG_CODE_List1	Task 1
…	…	…	…	…	…	…	…
Obj_ID N	First_Time N	Last_Time N	Spend_Time N	First_LSG_CODE N	Last_LSG_CODE N	LSG_CODE_List N	Task N

Table 2. Flight path and trajectory grid representation data structure.

And when organizing dynamic airspace data, it is necessary to identify the duration, and the data structure expressed by 3D subdivision is shown in Table 3.

Region ID	Region type	Grid code west boundary	Grid code north boundary	Grid code east boundary	Grid code south boundary	Grid boundary sequence	start time point	duration
Reg_ID 1	TYPE 1	LSGW_CODE1	LSGN_CODE1	LSGE_CODE1	LSGS_CODE 1	LSG_CODE_List 1	First_Time1	Time_Last 1
Reg_ID 2	TYPE 2	LSGW_CODE2	LSGN_CODE2	LSGE_CODE2	LSGS_CODE 2	LSG_CODE_List 2	First_Time1	Time_Last 2
…	…	…	…	…	…	…	…	…
Reg_ID N	TYPE 3	LSGW_CODEN	LSGN_CODEN	LSGE_CODEN	LSGW_CODEN	LSG_CODE_List N	First_Time1	Time_Last N

Table 3. Dynamic spatial grid subdivision expression data structure.

5. Conclusions

The dynamic airspace grid map based on GeoSOT-3D can uniformly subdivision the airspace into multi-scale grid, achieving effective integration of grids and entities. Through encoding and identification of aircraft and airspace, dynamic airspace grid map can quickly and automatically update and manage the dynamic airspace.

Acknowledgements

The research is supported by the Beijing Nova Program (No. 20240484563).

References

Bauranov, A., and Rakas, J., 2021. Designing airspace for urban air mobility: A review of concepts and approaches. *Progress in Aerospace Sciences* 125. doi: 10.1016/j.paerosci.2021.100726.

Davies, L., Vagapov, Y., Grout, V., Cunningham, S., and Anuchin, A. 2021. Review of Air Traffic Management Systems for UAV Integration into Urban Airspace. Paper presented at the 2021 28th International Workshop on Electric Drives: Improving Reliability of Electric Drives (IWED), 27-29 Jan. 2021.

Du, X., Lu, Z., and Wu, D., 2020. An intelligent recognition model for dynamic air traffic decision-making. *Knowledge*-Based *Systems* 199. doi: 10.1016/j.knosys.2019.105274.

Guan, X., Shi, H., Xu, D., Zhang, B., Wei, J., and Chen, J., 2024. The exploration and practice of low-altitude airspace flight service and traffic management in China. *Green Energy and Intelligent Transportation* 3 (2). doi: 10.1016/j.geits.2024.100149.

Han, B., Qu, T., Huang, Z., Wang, Q., and Pan, X., 2021. Emergency airport site selection using global subdivision grids. *Big Earth Data* 6 (3):276-93. doi: 10.1080/20964471.2021.1996866.

Han, B., Qu, T., and Jiang, J., 2025. GN-GCN: Grid neighborhood-based graph convolutional network for spatio-temporal *knowledge* graph reasoning. *ISPRS Journal of Photogrammetry and Remote Sensing* 220:728-39. doi: 10.1016/j.isprsjprs.2025.01.023.

Han, B., Qu, T., Tong, X., Jiang, J., Zlatanova, S., Wang, H., and Cheng, C., 2022. Grid-optimized UAV indoor path planning algorithms in a complex environment. *International Journal of Applied Earth Observation and Geoinformation* 111. doi: 10.1016/j.jag.2022.102857.

Han, B., Qu, T., Tong, X., Wang, H., Liu, H., Huo, Y., and Cheng, C., 2023. AugGKG: a grid-augmented geographic knowledge *graph* representation and spatio-temporal query model. *International Journal of Digital Earth* 16 (2):4934-57. doi: 10.1080/17538947.2023.2290569.

Hearn, T. A., Kotwicz Herniczek, M. T., and German, B. J., 2023. Conceptual Framework for Dynamic Optimal Airspace Configuration for Urban Air Mobility. *Journal of Air Transportation* 31 (2):68-82. doi: 10.2514/1.D0327.

Huang, H., Su, J., and Wang, F.-Y., 2024. The Potential of Low-Altitude Airspace: The Future of Urban Air Transportation. *IEEE* Transactions *on Intelligent Vehicles* 9 (8):5250-4. doi: 10.1109/tiv.2024.3483889.

Kwon, J., Kim, Y., and Choi, S.-H., 2018. Airspace map design to implement customer-friendly service on unmanned aerial vehicles. *Spatial Information Research* 27 (1):87-95. doi: 10.1007/s41324-018-0205-z.

Li, J., Wang, T., Savai, M., Hwang, I. J. J. o. g., control,, and dynamics, 2010. Graph-based algorithm for dynamic airspace configuration. 33 (4):1082-94.

LIAO, X., XU, C., and YE, H., 2024. Benefits and challenges of constructing low-altitude air route network infrastructure for developing low-altitude economy. *Bulletin* of *Chinese Academy of Sciences* 39 (11):1966-81.

Liu, Y., Zhang, X., Huang, F., Zhang, B., and Li, Z., 2022. Cross-Attentional Spatio-Temporal Semantic Graph Networks for Video Question Answering. *IEEE Trans Image Process* 31:1684-96. doi: 10.1109/TIP.2022.3142526.

Pang, B., Dai, W., Ra, T., and Low, K. H. 2020. A Concept of Airspace Configuration and Operational Rules for UAS in Current Airspace. Paper presented at the 2020 AIAA/IEEE 39th Digital Avionics Systems Conference (DASC), 11-15 Oct. 2020.

Sainz Carreño, Á., Pariente Concejo, A., Tena Diaz, J. A., Chornique Sanchez, J., Evans, A. D., and Anand, A. 2023. Simulating the use of Dynamic Airspace Reconfiguration to Support Integrated Crewed and Uncrewed Aircraft Operations. Paper presented at the AIAA AVIATION 2023 Forum.

Xie, Y., Gardi, A., Liang, M., and Sabatini, R., 2024. Hybrid AI-based 4D trajectory management system for dense low altitude operations and Urban Air Mobility. *Aerospace* Science *and Technology* 153. doi: 10.1016/j.ast.2024.109422.

Zhai, W., Han, B., Li, D., Duan, J., and Cheng, C., 2021. A low-altitude public air route network for UAV management constructed by global subdivision grids. *PLoS One* 16 (4):e0249680. doi: 10.1371/journal.pone.0249680.

Zhao, Z., Zhang, L., Zhou, R., Li, G., Wang, S., Liu, T., and Wu, Y., 2024. A flight risk field model for advanced low-altitude transportation system using field theory. Transportation *Research Part A: Policy and Practice* 190. doi: 10.1016/j.tra.2024.104268.